High resolution spatiotemporal distribution of rainfall seasonality and extreme events based on a 12-year TRMM time series

Bodo Bookhagen, Geography Department, UC Santa Barbara, Santa Barbara, CA 93106-4060
bodo@icess.ucsb.edu

Methods and Data

Comparison of mean annual surface rainfall (1998 to 2007) from TRMM product 2A25 (precipitation radar, PR) and TRMM product 2B31 (combined passive microwave, TMI and precipitation radar, PR). In general, both dataset agree well, but product 2A25 indicates some very high rainfall amounts (> 8 m/y) that are not supported by ground-based rain gauges.

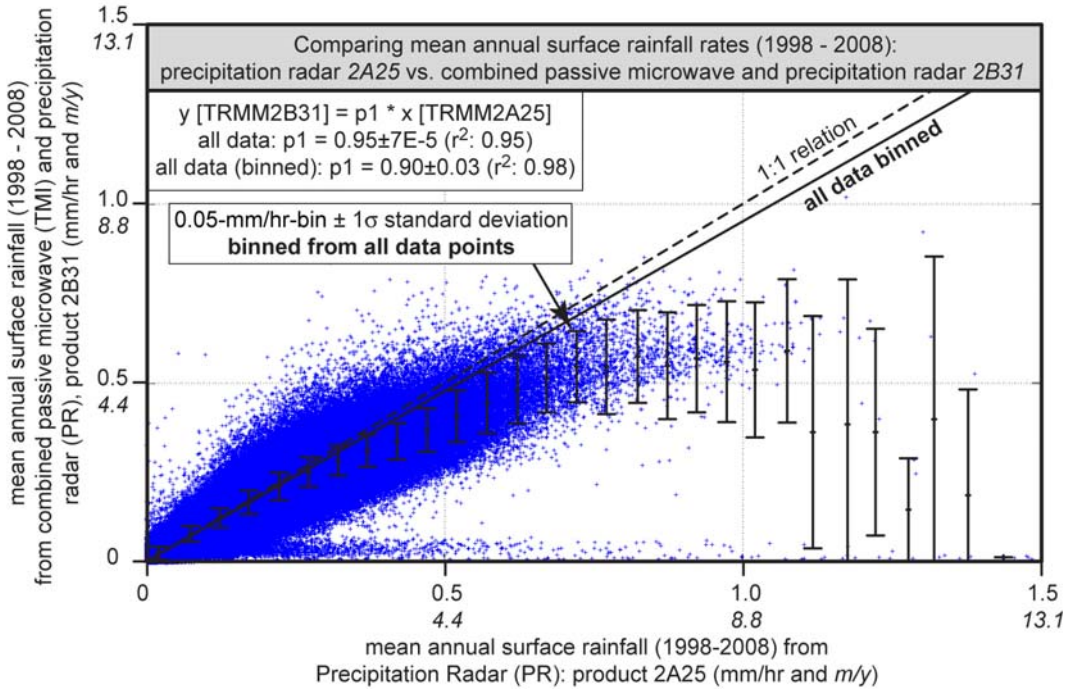

Figure DR 1: Comparison of TRMM product 2A25 and 2B31. The precipitation radar (PR) product 2A25 has slightly higher values than the combined passive microwave (TMI) and precipitation radar (PR) product 2B31. Black dashed line indicate 1:1 relation, black line indicates a weighted linear fit to all 0.5-mm/hr-binned data points (r^2 = 0.98). Black whiskers are 1-σ standard deviations for rainfall amounts in 0.05 mm/hr bins. A linear fit to all data points results in similar parameters (y[TRMM2B31] = 0.95±7E-5 * x [TRMM2A25] with r2=0.95) and is not shown in this graph. See Figure DR2 and DR3 for delineation between land and ocean.

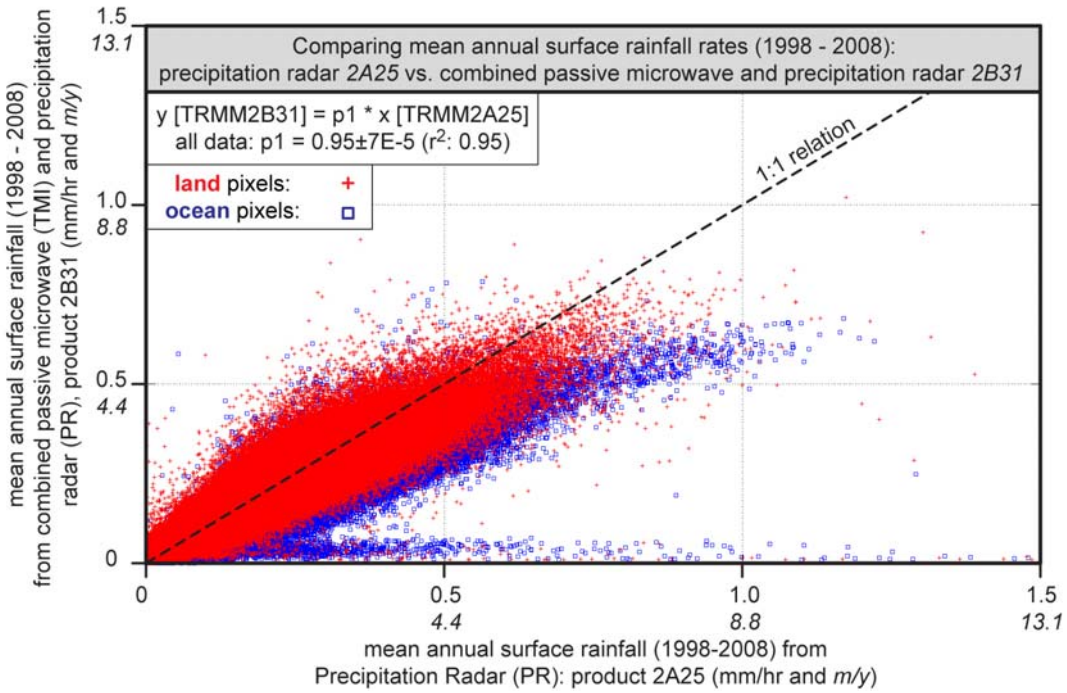

Figure DR 2: Comparison of precipitation radar (PR) product 2A25 and combined passive microwave and precipitation radar (PR) product 2B31 over land (red crosses) and ocean (blue squares). Shown here are all data pixels. Both data indicate that product 2A25 results in higher surface rainfall amounts and especially some ocean pixels have high surface-rainfall amounts in the TRMM product 2A25.

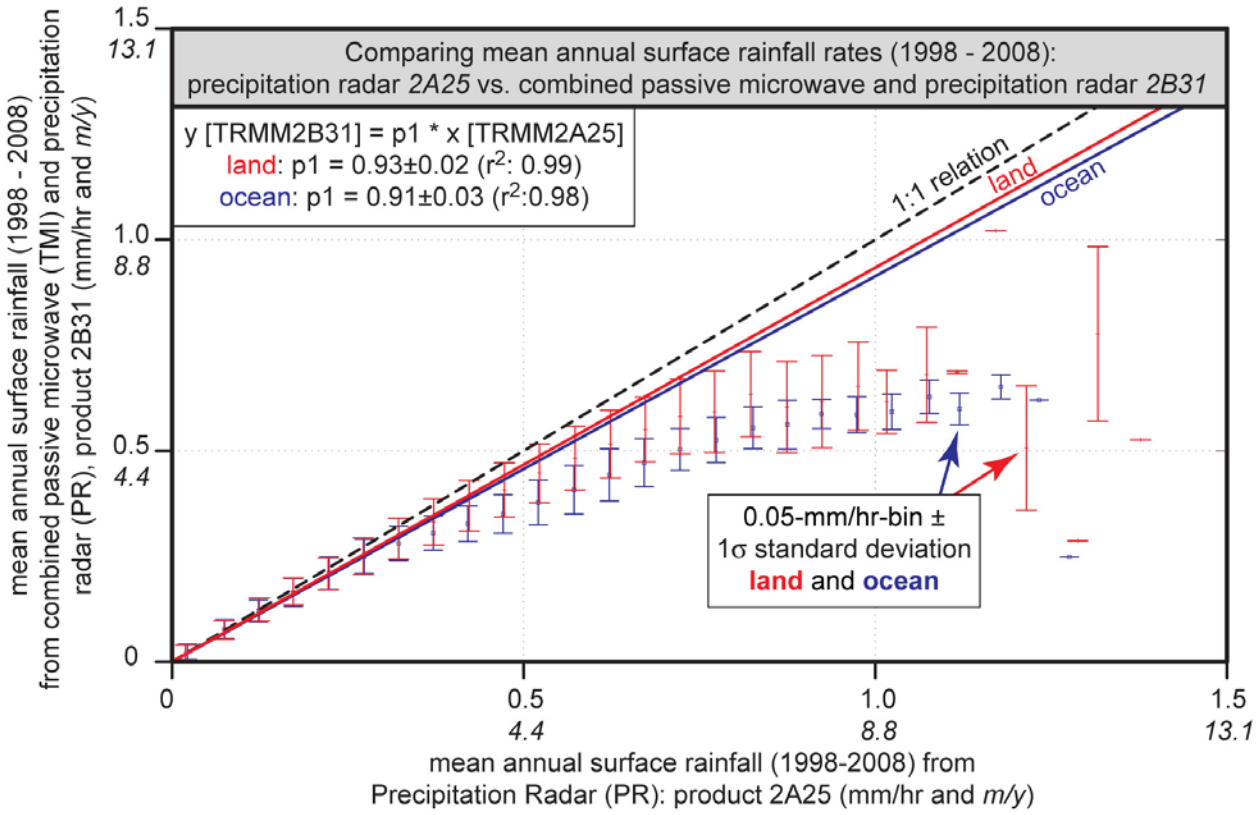

Figure DR 3: Comparison of mean annual surface rainfall amounts derived from precipitation radar (PR) product 2A25 and combined passive microwave (TMI) and precipitation radar (PR) product 2B31. Data were binned into 0.05 mm/hr steps and only the mean and their respective 1-σ standard deviation are shown here to avoid cluttering the figure; all data points are shown in Figure DR2. There is no significant difference in land and ocean rainfall amounts (red and blue lines). In general, surface rainfall between both dataset correlate very well up to 0.4 mm/hr (3.5 m/y), but there exists a large divergence at higher rainfall amounts. In some instances, product 2A25 results in (unrealistically) high rainfall amounts in excess of 8 m/y for a 0.05x0.05º grid cell. These are not supported by ground-based rain gauges and exceed the amount of rain falling in a ~5x5km grid cell. I find identical linear fitting parameters between TRMM product 2A25 and the GPCC [*Schneider et al.*, 2008] data: y [TRMM2A25 in mm/y] = x [TRMM2A25 in mm/hr] * (1/0.8635) ± (1/0.0082) with r^2 = 0.80 [*Nesbitt and Anders*, 2009]. However, TRMM product 2A25 has numerous pixels with high annual rainfall amounts above 8 m/y (Figure DR3). The largest discrepancies between PR product 2A25 and combined TMI and PR product 2B31 are in the southeastern Pacific and southeastern Atlantic (Figure DR7).

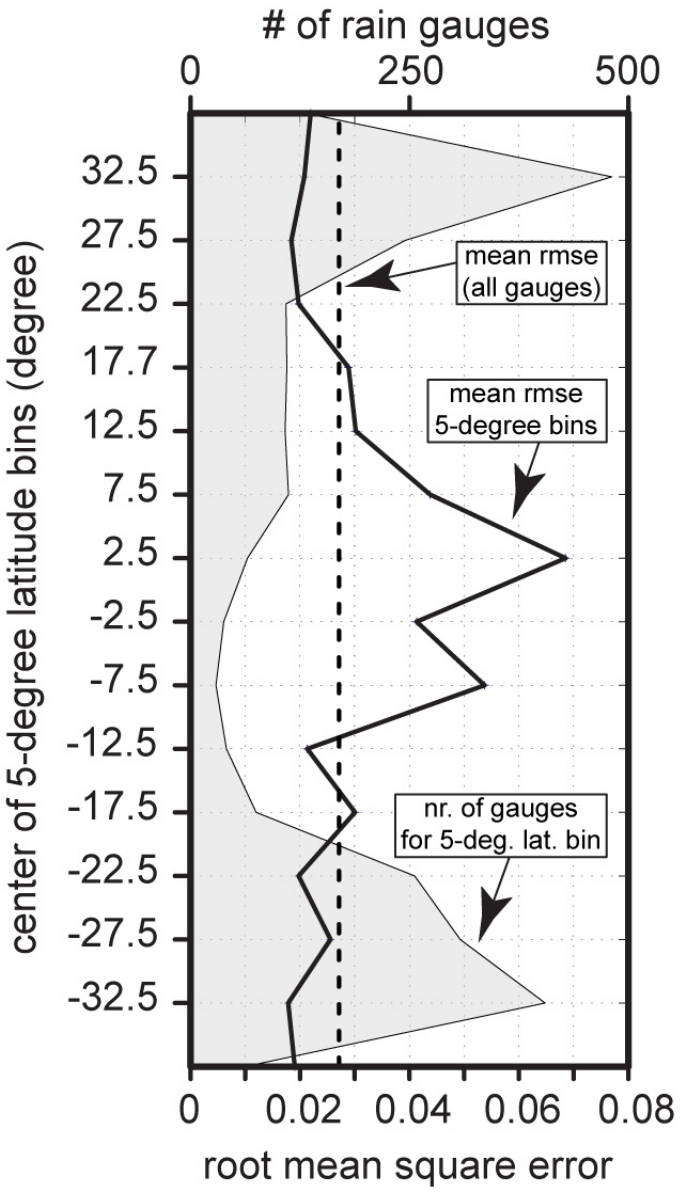

Figure DR 4: Latitudinal variations in calibration error and number of rain gauges (GPCC). There exists a large number of stations in the densely populated subtropical northern and southern latitudes (±30º) and these regions have a generally low root mean square error during the calibration procedure. The less dense station coverage in the tropics as well as short-lived convective rainfall leads to higher root mean square errors.

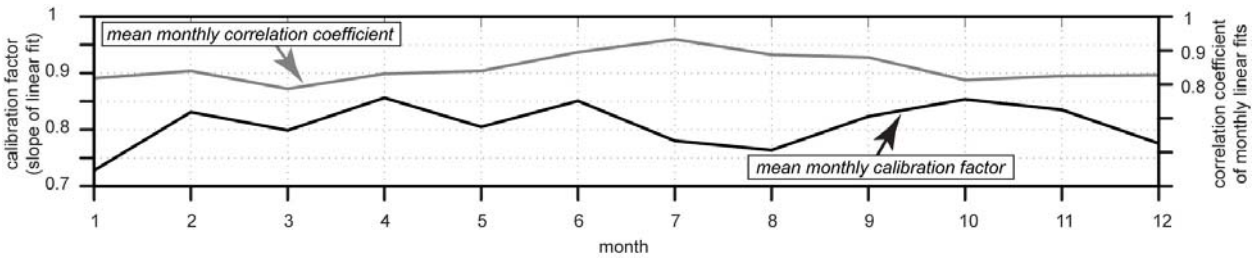

Figure DR 5: Monthly calibration factors (black) and their corresponding correlation coefficients (gray). Monthly data were averaged from 1998 to 2007 (10 years) and show generally high correlation coefficients with maximum coefficients in July. These calibration factors were used to convert instantaneous rainfall intensities (mm/hr) to mean monthly rainfall amounts (mm/month.

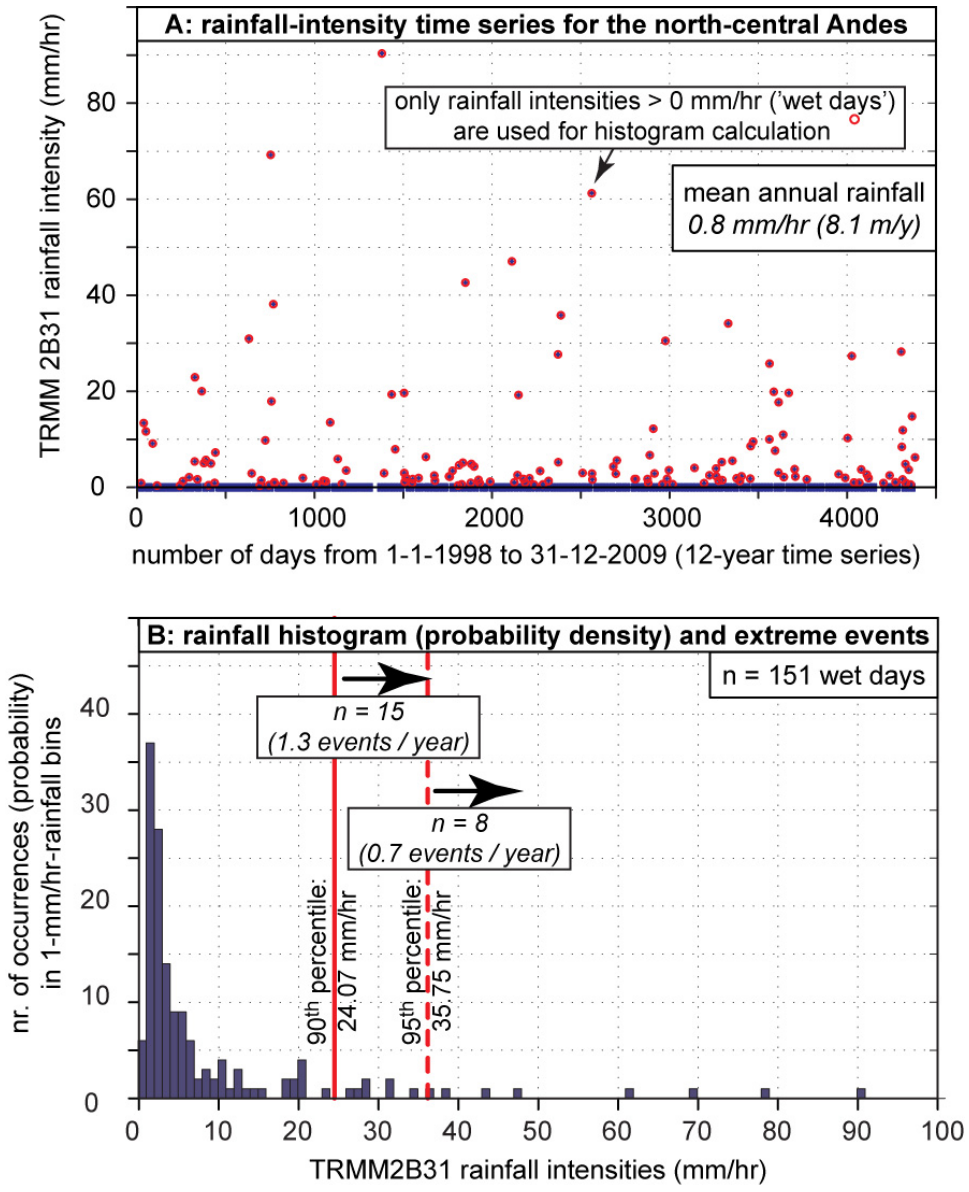

Figure DR 6: Example of calculating the 90th percentile from a characteristic setting in the north-central Andes with a mean rainfall intensity of 0.8 m/hr (8.1 m/y). (A) Time series in daily steps and rainfall intensities. For the probability density calculation, only rainfall intensities > 0 mm/hr are chosen ('wet days'). (B) Probability density (or histogram) of the wet days and the corresponding 90th and 95th percentiles. Extreme events are defined as having a rainfall intensity at or above the 90th percentile.

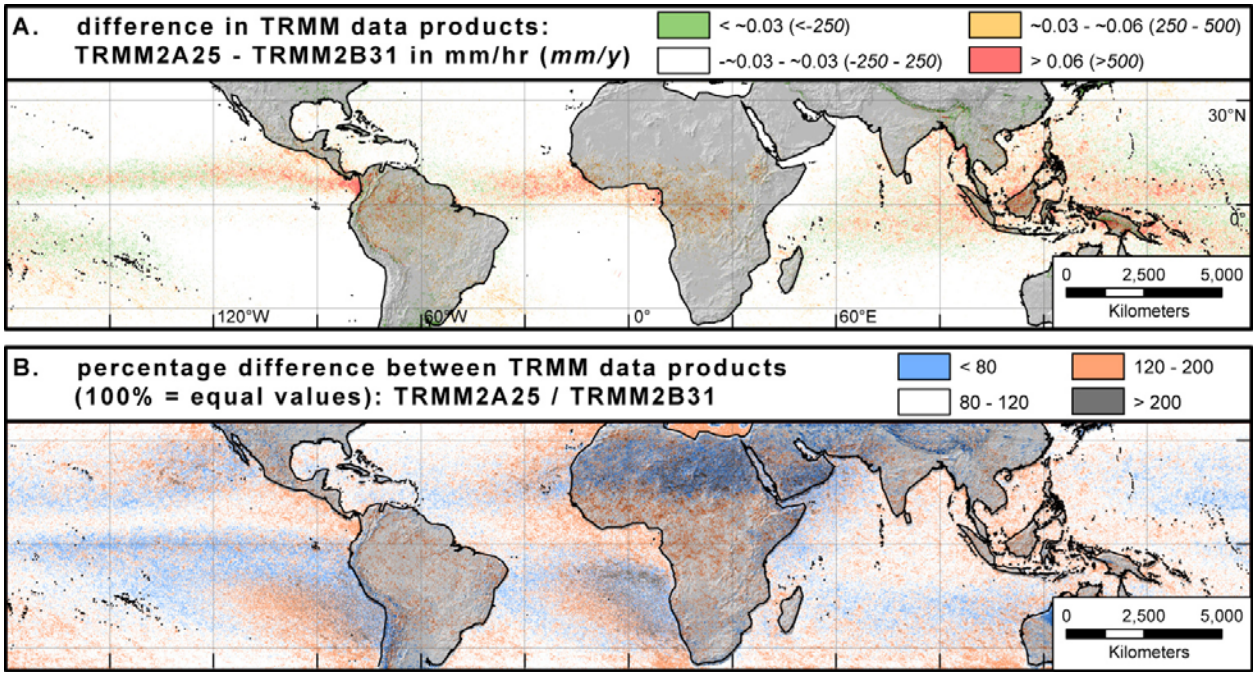

Figure DR 7: Difference between TRMM Precipitation Radar (PR) product 2A25 [*Nesbitt and Anders*, 2009] and TRMM combined microwave imager (TMI) and Precipitation Radar (PR) product 2B31. The absolute differences in surface rainfall are low (±0.03 mm/hr or ±250 mm/y) in most geographic regions as indicated by the white background color. TRMM2A25 produces significantly higher surface rainfall amounts in tropical Central America, Africa, and Indonesia. TRMM2B31 has higher surface rainfall amounts in the southwestern tropical Pacific and in the Ganges Plains (India). There is no consistent bias between ocean and land coverages. Lower panel (B) shows differences in percentage: Surface rainfall amounts are consistent within 20% in the white areas. Light blue areas indicate regions where TRMM2B31 are lower by more than 20%, and orange regions where TRMM2A25 is higher by 20-100% (factor 1.2 – 2). Dark gray colors outline areas where TRMM2A25 is more than twice as high as TRMM2B31.

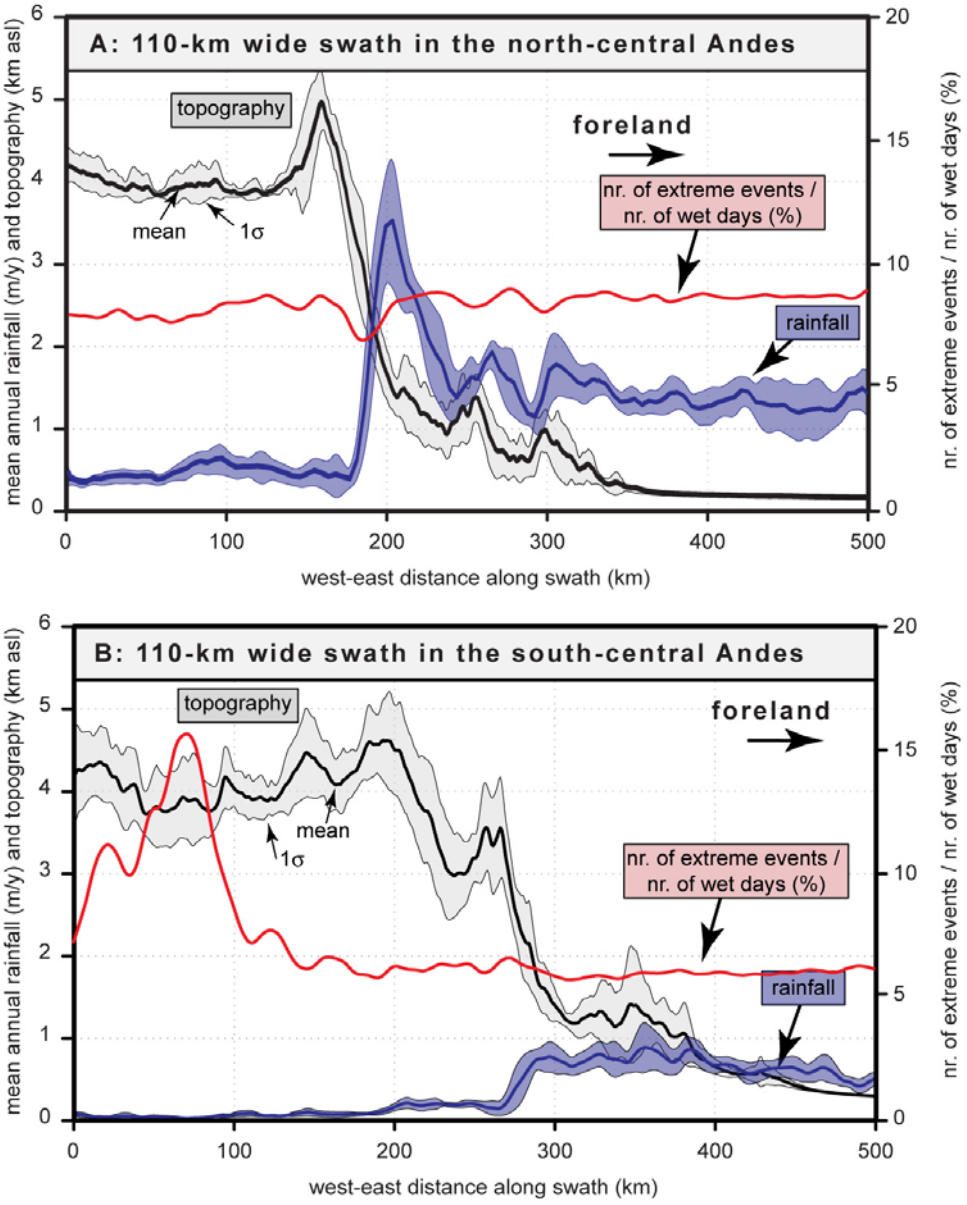

Figure DR 8: 110-km wide and 500-km long swath profiles for the northern and southern central Andes (see Figure 5 for swath location). Shown here is topography (gray), rainfall (blue), and the ratio of number of extreme events to number of wet days in percent (red). In the northern central Andes (A) between 8 to 9% of all rainfall events occur in the 90th percentile. In contrast, in the southern-central Andes (B) only 5 to 6% of all rainfall events are extreme events. The higher percentage (~15%) at high elevation in the south-central Andes are caused by rainfall storms that propagated from the Pacific Ocean into the western Altiplano-Puna Plateau region [e.g., *Bookhagen and Strecker*, 2010; *Garreaud et al.*, 2003].

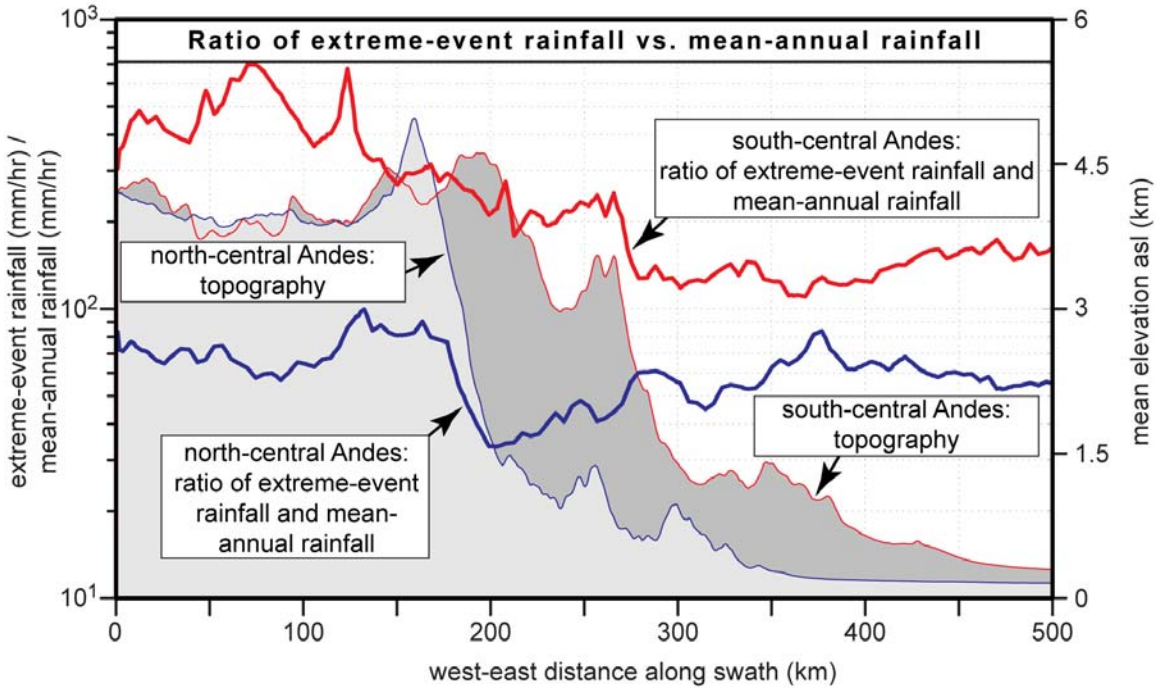

Figure DR 9: Ratio of extreme-event rainfall and mean-annual rainfall for the northern and southern-central Andes. The ratio indicates the increase factor from mean-annual rainfall (mm/hr) to extreme-event rainfall (mm/hr): A value of 100 corresponds to 100-times higher extreme-event rainfall than mean-annual rainfall. Note the logarithmic scale of the Y axis. In general, the ratio in the northern central Andes varies by a factor of two (blue solid line). In contrast, the southern-central Andes have a significant higher ratio at low elevations that increases ~7-fold in the high elevation regions of the southern Altiplano-Puna Plateau (red line).

References

Bookhagen, B., and M. R. Strecker (2010), Modern Andean rainfall variation during ENSO cycles and its impact on the Amazon Basin, in *Neogene history of Western Amazonia and its significance for modern diversity*, edited by C. Hoorn, et al., Blackwell Publishing, Oxford, U.K.

Garreaud, R., et al. (2003), The climate of the Altiplano: observed current conditions and mechanisms of past changes, *Palaeogeography Palaeoclimatology Palaeoecology*, *194*(1-3), 5-22.

Nesbitt, S. W., and A. M. Anders (2009), Very high resolution precipitation climatologies from the Tropical Rainfall Measuring Mission precipitation radar, *Geophysical Research Letters*, *36*.

Schneider, U., et al. (2008), Global Precipitation Analysis Products of the GPCC. Global Precipitation Climatology Centre (GPCC), *Deutscher Wetter Dienst (DWD), Internet Publikation*, *1*(12).